

Configurational entropy of charged AdS black holes

Chong Oh Lee*

Department of Physics, Kunsan National University, Kunsan 573-701, Korea

When we consider charged AdS black holes in higher dimensional spacetime and a molecule number density along coexistence curves is numerically extended to higher dimensional cases. It is found that a number density difference of a small and large black holes decrease as a total dimension grows up. In particular, we find that a configurational entropy is a concave function of a reduced temperature and reaches a maximum value at a critical (second-order phase transition) point. Furthermore, the bigger a total dimension becomes, the more concave function in a configurational entropy while the more convex function in a reduced pressure.

I. INTRODUCTION

It has been found that there is a first-order phase transition in the Schwarzschild-AdS black hole from analogy between black hole and standard thermodynamic system [1]. It has been suggested that the critical behavior of charged AdS black holes remind Van der Waals liquid-gas phase transition [2, 3]. Thermodynamics of black holes in the extended space has been recently investigated by treating the cosmological constant as the thermodynamic pressure [4]. It has been found that the thermodynamic pressure of charged AdS black holes is proportional to their thermodynamic volume [5]. The $P - V$ criticality of charged AdS black holes in the extended space has been investigated [6, 7]

A present-day concept of configurational entropy has been suggested in Ref. [8] in search for the informational entropy in the context of communication theory. It was recently obtained in Ref. [9] through investigation of measure of ordering in field configuration space for spatially localized energy solutions of nonlinear models and used to study instability of a variety of objects [10–17].

The number density of black hole molecules was recently introduced in Ref. [18] for investigation of measure of the microscopic degrees of freedom of black holes. It was extensively studied for $f(R)$ AdS black holes and Gauss-Bonnet AdS black holes [19] and for the generalization of charged AdS black hole specific volume and number density [20].

The paper is organized as follows: in the next section we investigate configurational entropy in charged AdS black holes in higher dimensional spacetime. In the four-dimensional case, we explicitly present the configurational entropy. In the five-dimensional/six-dimensional case, its numerical result is given. In the last subsection we discuss their thermodynamic properties. In the last section we give our conclusion.

II. CONFIGURATIONAL ENTROPY

In statistical thermodynamics the most general formula between the entropy and the set of probabilities of their microscopic states is given as the Boltzmann-Gibbs entropy S_{BG}

$$S_{BG} = -k_B \sum p_i \ln p_i, \quad (2.1)$$

with $\sum p_i = 1$ where k_B is the Boltzmann constant, and p_i is the probability of a microstate. Each microstate has equal probability as the following

$$p_i = \frac{1}{W}, \quad (2.2)$$

where W is the number of microstates. Then the Boltzmann-Gibbs entropy S_{BG} (2.1) reduces to

$$S_{BG} = k_B \ln W, \quad (2.3)$$

where W is treated as the number of possible configurations at the given energy, and the Boltzmann-Gibbs entropy S_{BG} (2.3) becomes the configurational entropy in the microcanonical ensemble. Especially, supposing there are two different molecules with the total number of molecules N_0 , then the number of one type of molecule is N_1 and the number of another type of molecule N_2 . The configurational entropy S is written as

$$S = k_B \ln W = k_B \ln \left(\frac{N_0!}{N_1! N_2!} \right), \quad (2.4)$$

which leads to

$$S = k_B (N_0 \ln N_0 - N_1 \ln N_1 - N_2 \ln N_2), \quad (2.5)$$

by employing sterling's approximation $\ln N! \approx N \ln N$. Since the effective number density n for the AdS black hole is given as [6, 7]

$$n = \frac{N}{V} = \frac{1}{2l_P^2 r_h} \quad (2.6)$$

where V is the thermodynamic volume and l_P is Planck length

$$l_P = \sqrt{\hbar G/c^3}, \quad (2.7)$$

the configurational entropy of charged AdS black holes per unit volume s_{conf} reduces to

$$s_{conf} = - \left[n_1 \ln \left(\frac{n_1}{n_1 + n_2} \right) + n_2 \ln \left(\frac{n_2}{n_1 + n_2} \right) \right] \quad (2.8)$$

* cohlee@gmail.com

by using geometric units $G = c = k_B = \hbar = 1$.

The charged AdS black hole metric in higher dimensional spacetime is given as

$$ds^2 = -f(r)dt^2 + \frac{dr^2}{r^2} + r^2 d\Omega_{d-2}^2. \quad (2.9)$$

with

$$f(r) = 1 - \frac{m}{r^{d-3}} + \frac{q^2}{r^{2(d-3)}} + \frac{r^2}{l^2}, \quad (2.10)$$

where parameter m relates to the ADM mass M , which is identified with enthalpy H ($M \equiv H = U + PV$) [4]

$$M \equiv H = \frac{\pi^{\frac{d-1}{2}}(d-2)m}{8\pi\Gamma(\frac{d-1}{2})}, \quad (2.11)$$

and parameter q relates to the black hole charge Q [2, 3]

$$Q = \frac{\pi^{\frac{d-1}{2}}\sqrt{2(d-2)(d-3)q}}{4\pi\Gamma(\frac{d-1}{2})}. \quad (2.12)$$

One may treat the cosmological constant Λ as the thermodynamic pressure P

$$P = -\frac{\Lambda}{8\pi} = \frac{(d-1)(d-2)}{8\pi l^2}, \quad (2.13)$$

and its conjugate quantity as the thermodynamic volume [5].

$$V = \frac{2\pi^{\frac{d-1}{2}}r_h^{d-1}}{\Gamma(\frac{d-1}{2})} \quad (2.14)$$

The d -dimensional black hole temperature T can read

$$T = \frac{1}{4\pi r_h} \left[(d-3) + \frac{16\pi P}{d-2} r_h^2 - \frac{(d-3)q^2}{r_h^{2(d-3)}} \right], \quad (2.15)$$

which leads to the thermodynamic pressure P

$$P = \frac{(d-2)T}{4r_h} - \frac{(d-2)(d-3)}{16\pi r_h^2} + \frac{(d-2)(d-3)q^2}{16\pi r_h^{2(d-2)}}. \quad (2.16)$$

Employing the Legendre transform of enthalpy $\tilde{G} = H - TS$, the Gibbs free energy \tilde{G} is given as

$$\tilde{G} = \frac{\pi^{\frac{d-1}{2}}}{8\pi\Gamma(\frac{d-1}{2})} \left[r_h^{d-3} - \frac{16\pi P r_h^{d-1}}{(d-1)(d-2)} + \frac{(2d-5)q^2}{r_h^{d-3}} \right]. \quad (2.17)$$

The specific volume v of the black hole fluid is identified with the horizon radius of the black hole through comparing with the Van der Waals equation [6, 7]

$$v = \frac{4l^{\frac{d-2}{2}}}{d-2}, \quad (2.18)$$

and the equation of state is given as

$$P = \frac{T}{v} - \frac{d-3}{\pi(d-2)v^2} + \frac{4^{2d-5}(d-3)q^2}{4\pi(d-2)^{2d-5}v^{2(d-2)}}. \quad (2.19)$$

The critical point is obtained by solving the following two equations

$$\frac{\partial P}{\partial v} = 0, \quad \frac{\partial^2 P}{\partial v^2} = 0, \quad (2.20)$$

which leads to

$$P_c = \frac{(d-3)^2}{\pi(d-2)^2 v_c^2}, \quad (2.21)$$

$$T_c = \frac{4(d-3)^2}{\pi(d-2)(2d-5)v_c}, \quad (2.22)$$

$$v_c = \frac{4}{d-2} \left[(d-2)(2d-5)q^2 \right]^{\frac{1}{2(d-3)}}, \quad (2.23)$$

$$\tilde{G}_c = \frac{\pi^{\frac{d-1}{2}}\sqrt{(d-2)(2d-5)q}}{2\pi\Gamma(\frac{d-1}{2})(d-1)}. \quad (2.24)$$

Employing the the reduced physical parameters as

$$p = \frac{P}{P_c}, \quad \tau = \frac{T}{T_c}, \quad \nu = \frac{v}{v_c}, \quad G = \frac{\tilde{G}}{\tilde{G}_c}, \quad (2.25)$$

the Gibbs free energy (2.17) is written as

$$G = \frac{1}{4} \left[(d-1)\nu^{d-3} - \frac{(d-3)^2 p \nu^{d-1}}{d-2} + \frac{d-1}{(d-2)\nu^{d-3}} \right] \quad (2.26)$$

and the equation of state is

$$p = \frac{4(d-2)\tau}{(2d-5)\nu} - \frac{d-2}{(d-3)\nu^2} + \frac{1}{(d-3)(2d-5)\nu^{2(d-2)}}, \quad (2.27)$$

which leads to

$$\tau = \frac{(2d-5)p\nu}{4(d-2)} - \frac{2d-5}{4(d-3)\nu} - \frac{1}{4(d-2)(d-3)\nu^{2d-5}}. \quad (2.28)$$

Since the first-order phase transition occurs between the small and large black hole along the coexistence curve except the critical point $\tau = \tau_c$, the two states have the same Gibbs free energy, and Eqs. (2.26) and (2.28) are written as

$$\begin{aligned} G_1 &= \frac{1}{4} \left[(d-1)\nu_1^{d-3} - \frac{(d-3)^2 p \nu_1^{d-1}}{d-2} + \frac{d-1}{(d-2)\nu_1^{d-3}} \right], \\ &= \frac{1}{4} \left[(d-1)\nu_2^{d-3} - \frac{(d-3)^2 p \nu_2^{d-1}}{d-2} + \frac{d-1}{(d-2)\nu_2^{d-3}} \right] \\ &= G_2, \end{aligned} \quad (2.29)$$

$$\begin{aligned} \tau &= \frac{(2d-5)p\nu_1}{4(d-2)} - \frac{2d-5}{4(d-3)\nu_1} - \frac{1}{4(d-2)(d-3)\nu_1^{2d-5}}, \\ &= \frac{(2d-5)p\nu_2}{4(d-2)} - \frac{2d-5}{4(d-3)\nu_2} - \frac{1}{4(d-2)(d-3)\nu_2^{2d-5}}. \end{aligned} \quad (2.30)$$

A. The four-dimensional case

In the case of $d = 4$, the above Eqs. (2.29) and (2.30) reduce to [18, 19]

$$\frac{p\nu_1^4 - 6\nu_1^2 - 3}{8\nu_1} = \frac{p\nu_2^4 - 6\nu_2^2 - 3}{8\nu_2}, \quad (2.31)$$

$$\frac{3p\nu_1^4 + 6\nu_1^2 - 1}{8\nu_1^3} = \frac{3p\nu_2^4 + 6\nu_2^2 - 1}{8\nu_2^3}, \quad (2.32)$$

$$2\tau = \frac{3p\nu_1^4 + 6\nu_1^2 - 1}{8\nu_1^3} + \frac{3p\nu_2^4 + 6\nu_2^2 - 1}{8\nu_2^3}. \quad (2.33)$$

For convenience, we now employ the parameters as the following

$$x = \nu_1 + \nu_2, \quad y = \nu_1\nu_2, \quad (2.34)$$

and the above Eqs. (2.31)~(2.33) are written as

$$-px^2y + py^2 + 6y - 3 = 0, \quad (2.35)$$

$$2py^3 + x^2 - 6y^2 - y = 0, \quad (2.36)$$

$$-3pxy^3 + x^3 - 6xy^2 - 3xy + 16\tau y^3 = 0 \quad (2.37)$$

These equations can be analytically solved, and the corresponding reduced pressure p is obtained as

$$p = \frac{2^{\frac{4}{3}}\tau^2(-\tau + \sqrt{\tau^2 - 2})^{\frac{2}{3}}}{[2^{\frac{1}{3}} + (-\tau + \sqrt{\tau^2 - 2})^{\frac{2}{3}}]^2}, \quad (2.38)$$

which is shown as red solid curve in Fig. 1.

Introducing the number density of black hole molecules $n = 1/v$, we have

$$\begin{aligned} \frac{n_1 - n_2}{n_c} &= \frac{\nu_2 - \nu_1}{\nu_1\nu_2} = \frac{x^2 - 4y}{y} = \sqrt{6 - 6\sqrt{p}} \\ &= \sqrt{6 - \frac{6 \times 2^{\frac{2}{3}}\tau(-\tau + \sqrt{\tau^2 - 2})^{\frac{1}{3}}}{2^{\frac{1}{3}} + (-\tau + \sqrt{\tau^2 - 2})^{\frac{2}{3}}}}. \end{aligned} \quad (2.39)$$

which is shown as red solid curve in Fig. 2. Here, n_1 and n_2 are explicitly calculated as

$$\begin{aligned} n_1 &= \frac{1}{v_1} = \frac{\sqrt{x^2 - 4y} + x}{2y} = \frac{(\sqrt{3 - \sqrt{p}} + \sqrt{3 - 3\sqrt{p}})\sqrt{p}}{\sqrt{2}}, \\ &= \frac{1}{\sqrt{2}} \left(\sqrt{3 - \frac{2^{\frac{2}{3}}\tau(-\tau + \sqrt{\tau^2 - 2})^{\frac{1}{3}}}{2^{\frac{1}{3}} + (-\tau + \sqrt{\tau^2 - 2})^{\frac{2}{3}}}} \right. \\ &\quad \left. + \sqrt{3 - \frac{3 \times 2^{\frac{2}{3}}\tau(-\tau + \sqrt{\tau^2 - 2})^{\frac{1}{3}}}{2^{\frac{1}{3}} + (-\tau + \sqrt{\tau^2 - 2})^{\frac{2}{3}}}} \right) \\ &\quad \times \frac{2^{\frac{2}{3}}\tau(-\tau + \sqrt{\tau^2 - 2})^{\frac{1}{3}}}{2^{\frac{1}{3}} + (-\tau + \sqrt{\tau^2 - 2})^{\frac{2}{3}}}, \end{aligned} \quad (2.40)$$

$$\begin{aligned} n_2 &= \frac{1}{v_2} = \frac{\sqrt{x^2 - 4y} - x}{2y} = \frac{(\sqrt{3 - \sqrt{p}} - \sqrt{3 - 3\sqrt{p}})\sqrt{p}}{\sqrt{2}}, \\ &= \frac{1}{\sqrt{2}} \left(\sqrt{3 - \frac{2^{\frac{2}{3}}\tau(-\tau + \sqrt{\tau^2 - 2})^{\frac{1}{3}}}{2^{\frac{1}{3}} + (-\tau + \sqrt{\tau^2 - 2})^{\frac{2}{3}}}} \right. \\ &\quad \left. - \sqrt{3 - \frac{3 \times 2^{\frac{2}{3}}\tau(-\tau + \sqrt{\tau^2 - 2})^{\frac{1}{3}}}{2^{\frac{1}{3}} + (-\tau + \sqrt{\tau^2 - 2})^{\frac{2}{3}}}} \right) \\ &\quad \times \frac{2^{\frac{2}{3}}\tau(-\tau + \sqrt{\tau^2 - 2})^{\frac{1}{3}}}{2^{\frac{1}{3}} + (-\tau + \sqrt{\tau^2 - 2})^{\frac{2}{3}}}. \end{aligned} \quad (2.41)$$

Substituting with the configurational entropy (2.8), we get

$$\begin{aligned} s_{conf} &= - \left[\frac{(\sqrt{3 - \sqrt{p}} + \sqrt{3 - 3\sqrt{p}})\sqrt{p}}{\sqrt{2}} \right. \\ &\quad \times \ln \left\{ \frac{1}{2} \left(1 + \frac{\sqrt{3 - 3\sqrt{p}}}{\sqrt{3 - \sqrt{p}}} \right) \right\} \\ &\quad \left. + \frac{(\sqrt{3 - \sqrt{p}} - \sqrt{3 - 3\sqrt{p}})\sqrt{p}}{\sqrt{2}} \right. \\ &\quad \left. \times \ln \left\{ \frac{1}{2} \left(1 - \frac{\sqrt{3 - 3\sqrt{p}}}{\sqrt{3 - \sqrt{p}}} \right) \right\} \right] \\ &= - \left[\frac{1}{\sqrt{2}} \left(\sqrt{3 - \frac{2^{\frac{2}{3}}\tau(-\tau + \sqrt{\tau^2 - 2})^{\frac{1}{3}}}{2^{\frac{1}{3}} + (-\tau + \sqrt{\tau^2 - 2})^{\frac{2}{3}}}} \right. \right. \\ &\quad \left. \left. + \sqrt{3 - \frac{3 \times 2^{\frac{2}{3}}\tau(-\tau + \sqrt{\tau^2 - 2})^{\frac{1}{3}}}{2^{\frac{1}{3}} + (-\tau + \sqrt{\tau^2 - 2})^{\frac{2}{3}}}} \right) \right. \\ &\quad \times \frac{2^{\frac{2}{3}}\tau(-\tau + \sqrt{\tau^2 - 2})^{\frac{1}{3}}}{2^{\frac{1}{3}} + (-\tau + \sqrt{\tau^2 - 2})^{\frac{2}{3}}} \\ &\quad \left. \times \ln \left\{ \frac{1}{2} \left(1 + \frac{\sqrt{3 - 3 \times \frac{2^{\frac{2}{3}}\tau(-\tau + \sqrt{\tau^2 - 2})^{\frac{1}{3}}}{2^{\frac{1}{3}} + (-\tau + \sqrt{\tau^2 - 2})^{\frac{2}{3}}}}}{\sqrt{3 - \frac{2^{\frac{2}{3}}\tau(-\tau + \sqrt{\tau^2 - 2})^{\frac{1}{3}}}{2^{\frac{1}{3}} + (-\tau + \sqrt{\tau^2 - 2})^{\frac{2}{3}}}}} \right) \right\} \right. \\ &\quad \left. + \frac{1}{\sqrt{2}} \left(\sqrt{3 - \frac{2^{\frac{2}{3}}\tau(-\tau + \sqrt{\tau^2 - 2})^{\frac{1}{3}}}{2^{\frac{1}{3}} + (-\tau + \sqrt{\tau^2 - 2})^{\frac{2}{3}}}} \right. \right. \\ &\quad \left. \left. - \sqrt{3 - \frac{3 \times 2^{\frac{2}{3}}\tau(-\tau + \sqrt{\tau^2 - 2})^{\frac{1}{3}}}{2^{\frac{1}{3}} + (-\tau + \sqrt{\tau^2 - 2})^{\frac{2}{3}}}} \right) \right. \\ &\quad \times \frac{2^{\frac{2}{3}}\tau(-\tau + \sqrt{\tau^2 - 2})^{\frac{1}{3}}}{2^{\frac{1}{3}} + (-\tau + \sqrt{\tau^2 - 2})^{\frac{2}{3}}} \\ &\quad \left. \times \ln \left\{ \frac{1}{2} \left(1 - \frac{\sqrt{3 - 3 \times \frac{2^{\frac{2}{3}}\tau(-\tau + \sqrt{\tau^2 - 2})^{\frac{1}{3}}}{2^{\frac{1}{3}} + (-\tau + \sqrt{\tau^2 - 2})^{\frac{2}{3}}}}}{\sqrt{3 - \frac{2^{\frac{2}{3}}\tau(-\tau + \sqrt{\tau^2 - 2})^{\frac{1}{3}}}{2^{\frac{1}{3}} + (-\tau + \sqrt{\tau^2 - 2})^{\frac{2}{3}}}}} \right) \right\} \right], \end{aligned} \quad (2.42)$$

which is shown as red solid curve in Fig. 3.

B. The five-dimensional case

As discussed in the previous section we will apply a similar analysis to the five-dimensional case.

$$\frac{p\nu_1^6 - 3\nu_1^4 - 1}{3\nu_1^2} = \frac{p\nu_2^6 - 3\nu_2^4 - 1}{3\nu_2^2}, \quad (2.43)$$

$$\frac{10p\nu_1^6 + 15\nu_1^4 - 1}{24\nu_1^5} = \frac{10p\nu_2^6 + 15\nu_2^4 - 1}{24\nu_2^5}, \quad (2.44)$$

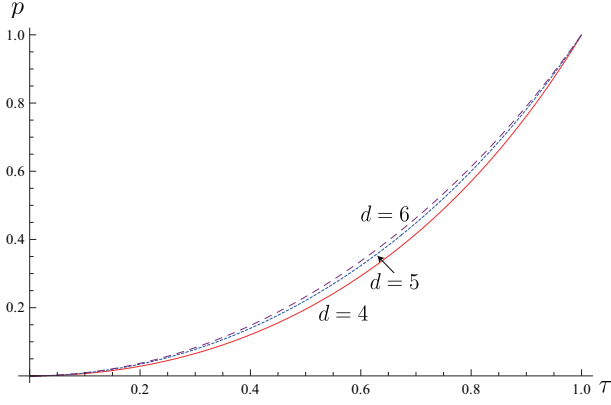


FIG. 1. Plot of the reduced pressure p as the function of the reduced temperature τ (red solid curve for $d = 4$, blue dotted curve for $d = 5$, and purple dashed curve for $d = 6$, respectively).

$$2\tau = \frac{10p\nu_1^6 + 15\nu_1^4 - 1}{24\nu_1^5} + \frac{10p\nu_2^6 + 15\nu_2^4 - 1}{24\nu_2^5}, \quad (2.45)$$

which leads to

$$-px^2y^2 + 2py^3 + 3y^2 - 1 = 0 \quad (2.46)$$

$$10py^5 + x^4 - 3x^2y - 15y^4 + y^2 = 0 \quad (2.47)$$

$$10pxy^5 - x^5 + 5x^3y + 15xy^4 - 5xy^2 + 48\tau y^5 = 0, \quad (2.48)$$

which is a complicated high-order polynomial equation and it is difficult to analyze exactly. However some numerical investigation can be employed and the reduced pressure p as the function of the reduced temperature τ is numerically calculated as blue dotted curve in Fig. 1. The number density difference of the small, and large black holes $(n_1 - n_2)/n_c$ as the function of the reduced temperature τ is numerically obtained as blue dotted curve in Fig. 2, and the configurational entropy s_{conf} as the function of the reduced temperature τ is numerically given as blue dotted curve in Fig. 3.

C. The six-dimensional case

We now apply similar numerical investigations to the six-dimensional case.

$$\frac{9p\nu_1^8 - 20\nu_1^6 - 5}{16\nu_1^3} = \frac{9p\nu_2^8 - 20\nu_2^6 - 5}{16\nu_2^3}, \quad (2.49)$$

$$\frac{21p\nu_1^8 + 28\nu_1^6 - 1}{48\nu_1^7} = \frac{21p\nu_2^8 + 28\nu_2^6 - 1}{48\nu_2^7}, \quad (2.50)$$

$$2\tau = \frac{21p\nu_1^8 + 28\nu_1^6 - 1}{48\nu_1^7} + \frac{21p\nu_2^8 + 28\nu_2^6 - 1}{48\nu_2^7}, \quad (2.51)$$

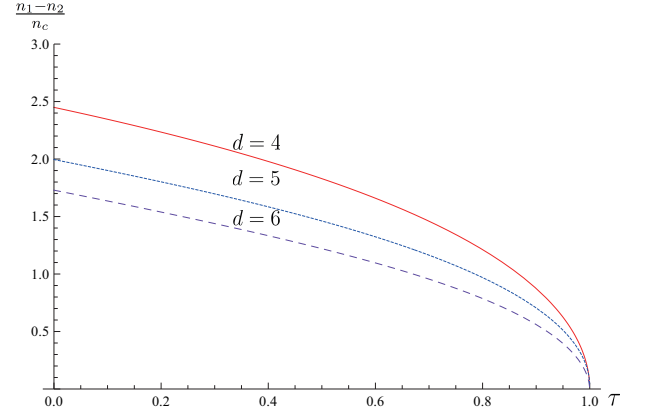


FIG. 2. Plot of the number density difference of the small and large black holes $(n_1 - n_2)/n_c$ as the function of the reduced temperature τ (red solid curve for $d = 4$, blue dotted curve for $d = 5$, and purple dashed curve for $d = 6$, respectively).

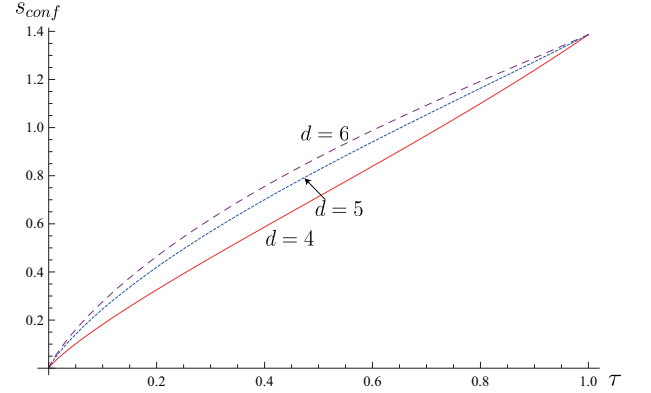


FIG. 3. Plot of the reduced configurational entropy s_{conf} as the function of the reduced temperature τ (red solid curve for $d = 4$, blue dotted curve for $d = 5$, and purple dashed curve for $d = 6$, respectively).

which leads to

$$\begin{aligned} -9px^4y^3 + 27px^2y^4 - 9py^5 + 20x^2y^3 \\ -5x^2 - 20y^4 + 5y = 0, \end{aligned} \quad (2.52)$$

$$21py^7 + x^6 - 5x^4y + 6x^2y^2 - 28y^6 - y^3 = 0, \quad (2.53)$$

$$\begin{aligned} -21pxy^7 + x^7 - 7x^5y + 14x^3y^2 \\ -28xy^6 - 7xy^3 + 96\tau y^7 = 0, \end{aligned} \quad (2.54)$$

which is numerically solved and the reduced pressure p as the function of the reduced temperature τ , the number density difference of the small, and large black holes $(n_1 - n_2)/n_c$ as the function of the reduced temperature τ , and the configurational entropy s_{conf} as the function of the reduced temperature τ are given as purple dashed curve in Fig. 1, Fig. 2, and Fig. 3, respectively.

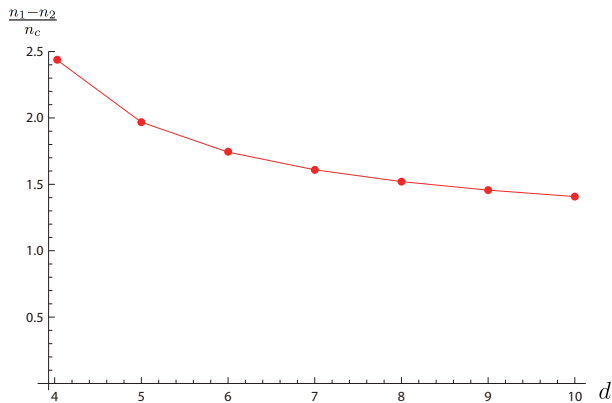


FIG. 4. Plot of the maximum number density difference of the small and large black holes $(n_1 - n_2)/n_c$ as the function of the total dimension d .

D. The thermodynamic properties

We now discuss the thermodynamic properties in charged AdS black holes in higher dimensional spacetime.

As shown in Fig. 1, and Fig. 2, as the reduced temperature τ grows up the reduced pressure p monotonically increases while the number density difference of the small, and large black holes $(n_1 - n_2)/n_c$ decreases. As shown in Fig. 3, the bigger the total dimension d becomes, the more concave function in the configurational entropy s_{conf} . Especially, as the reduced temperature τ grows up, s_{conf} monotonically increases, and reaches the maximum value at the critical (second-order phase transition) point. The maximum number density difference of the small and large black holes $(n_1 - n_2)/n_c$ at $\tau = 0$

is obtained as

$$\frac{n_1 - n_2}{n_c} = \left[(d - 2)(2d - 5) \right]^{\frac{1}{2(d-3)}}. \quad (2.55)$$

As shown in Fig. 4, it decreases as the total dimension d increases.

III. CONCLUSION

We considered higher dimensional charged AdS black holes and investigated the number density difference of the small and large black holes $(n_1 - n_2)/n_c$, and the reduced configurational entropy s_{conf} in the context of the molecule number density. We explicitly obtained the general form of maximum value of $(n_1 - n_2)/n_c$ at $\tau = 0$, and found that its maximum value decreases as the total dimension d increases. Especially, the configurational entropy s_{conf} monotonically increases as the reduced temperature τ grows up. It finally reaches a maximum value at a critical (second-order phase transition) point. This result is natural since in any system containing two different types of molecules, when they have the same number of molecules, the number of microstates W reaches maximum value. Furthermore, such result is consistent with that of the Van der Waals system. It was shown that the critical behaviour of charged AdS black holes coincides with those of the Van der Waals system [6]. In particular, when the second-order phase transition between liquid and gas occurs at the critical point, the distinction between the liquid and gas phases of the Van der Waals fluid is almost non-existent near the critical point and the molecules in the liquid and gas states are almost identical. Then, the number of microstates W becomes maximum.

-
- [1] S. W. Hawking and D. N. Page, Commun. Math. Phys. **87**, 577 (1983). doi:10.1007/BF01208266
- [2] A. Chamblin, R. Emparan, C. V. Johnson and R. C. Myers, Phys. Rev. D **60**, 064018 (1999) doi:10.1103/PhysRevD.60.064018 [hep-th/9902170].
- [3] A. Chamblin, R. Emparan, C. V. Johnson and R. C. Myers, Phys. Rev. D **60**, 104026 (1999) doi:10.1103/PhysRevD.60.104026 [hep-th/9904197].
- [4] D. Kastor, S. Ray and J. Traschen, Class. Quant. Grav. **26**, 195011 (2009) doi:10.1088/0264-9381/26/19/195011 [arXiv:0904.2765 [hep-th]].
- [5] M. Cvetič, G. W. Gibbons, D. Kubiznak and C. N. Pope, Phys. Rev. D **84**, 024037 (2011) doi:10.1103/PhysRevD.84.024037 [arXiv:1012.2888 [hep-th]].
- [6] D. Kubiznak and R. B. Mann, JHEP **1207**, 033 (2012) doi:10.1007/JHEP07(2012)033 [arXiv:1205.0559 [hep-th]].
- [7] S. Gunasekaran, R. B. Mann and D. Kubiznak, JHEP **1211**, 110 (2012) doi:10.1007/JHEP11(2012)110 [arXiv:1208.6251 [hep-th]].
- [8] C. E. Shannon, Bell Syst. Tech. J. **27**, 379 (1948) [Bell Syst. Tech. J. **27**, 623 (1948)].
- [9] M. Gleiser and N. Stamatopoulos, Phys. Lett. B **713**, 304 (2012) doi:10.1016/j.physletb.2012.05.064 [arXiv:1111.5597 [hep-th]].
- [10] M. Gleiser and N. Stamatopoulos, Phys. Rev. D **86**, 045004 (2012) doi:10.1103/PhysRevD.86.045004 [arXiv:1205.3061 [hep-th]].
- [11] M. Gleiser and D. Sowinski, Phys. Lett. B **727**, 272 (2013) doi:10.1016/j.physletb.2013.10.005 [arXiv:1307.0530 [hep-th]].
- [12] M. Gleiser and N. Graham, Phys. Rev. D **89**, no. 8, 083502 (2014) doi:10.1103/PhysRevD.89.083502 [arXiv:1401.6225 [astro-ph.CO]].
- [13] M. Gleiser and N. Jiang, Phys. Rev. D **92**, no. 4, 044046 (2015) doi:10.1103/PhysRevD.92.044046 [arXiv:1506.05722 [gr-qc]].
- [14] A. E. Bernardini and R. da Rocha, Phys. Lett. B **762**, 107 (2016) doi:10.1016/j.physletb.2016.09.023

- [arXiv:1605.00294 [hep-th]].
- [15] A. E. Bernardini, N. R. F. Braga and R. da Rocha, Phys. Lett. B **765**, 81 (2017) doi:10.1016/j.physletb.2016.12.007 [arXiv:1609.01258 [hep-th]].
- [16] R. Casadio and R. da Rocha, Phys. Lett. B **763**, 434 (2016) doi:10.1016/j.physletb.2016.10.072 [arXiv:1610.01572 [hep-th]].
- [17] N. R. F. Braga and R. da Rocha, Phys. Lett. B **767** (2017) 386 doi:10.1016/j.physletb.2017.02.031 [arXiv:1612.03289 [hep-th]].
- [18] S. W. Wei and Y. X. Liu, Phys. Rev. Lett. **115**, no. 11, 111302 (2015) Erratum: [Phys. Rev. Lett. **116**, no. 16, 169903 (2016)] doi:10.1103/PhysRevLett.116.169903, 10.1103/PhysRevLett.115.111302 [arXiv:1502.00386 [gr-qc]].
- [19] J. X. Mo and G. Q. Li, Phys. Rev. D **92**, no. 2, 024055 (2015) doi:10.1103/PhysRevD.92.024055 [arXiv:1604.07931 [gr-qc]].
- [20] Z. Wang, M. He, C. Fang, D. Sun and J. Deng, Gen. Rel. Grav. **49**, no. 4, 53 (2017) doi:10.1007/s10714-017-2216-9 [arXiv:1703.01387 [gr-qc]].